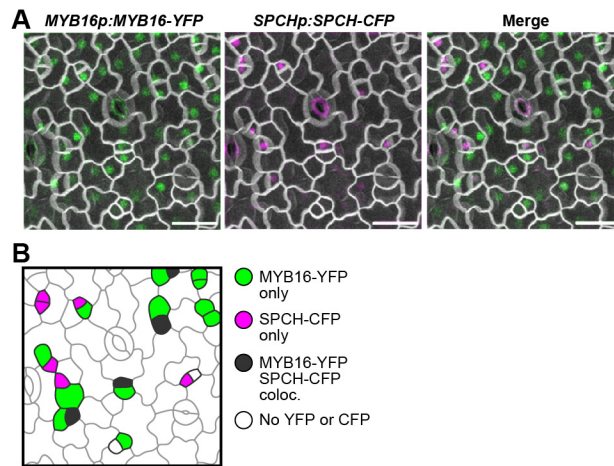


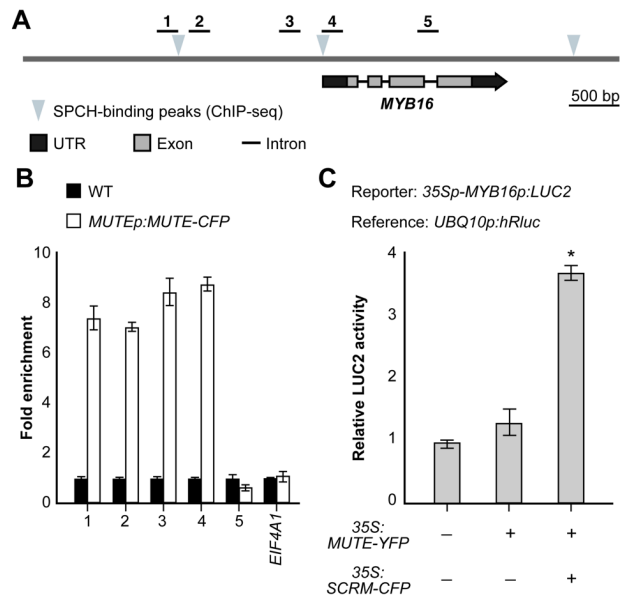
Supplemental Data. Yang et al. (2022). Misregulation of MYB16 expression causes stomatal cluster formation by disrupting polarity during asymmetric cell divisions. *Plant Cell*.



Supplemental Figure S1. MYB16 is preferentially localized to stomatal lineage ground cells (SLGCs). (Supports Figure 1)

(A) An example of images used for quantifying localization preference in **Figure 1B**. MYB16-YFP (green) and SPCH-CFP (magenta) in a wild-type (WT) 7 days post-germination (dpg) true leaf. Cell outline marked by RC12A-mCherry (gray). Scale bars, 20 μ m.

(B) A diagram showing meristemoid–SLGC pairs in **(A)**. The colors represent the fluorescent signals in the cells. Green, MYB16-YFP; magenta, SPCH-CFP; black, both MYB16 and SPCH; white, no signal detected.

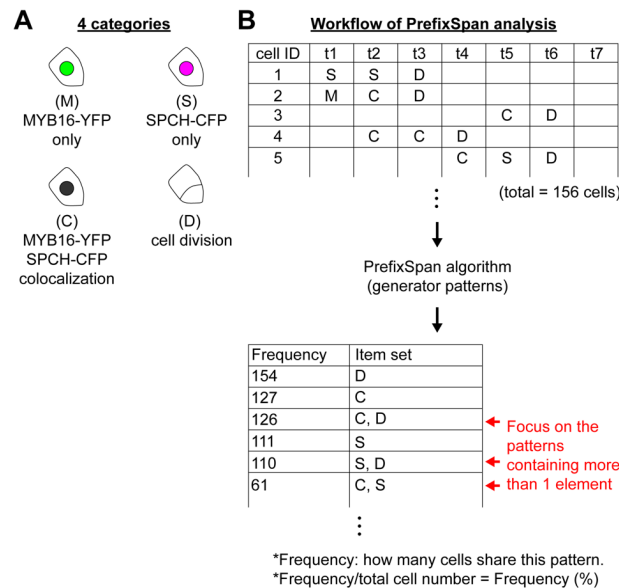


Supplemental Figure S2. MUTE binds to the MYB16 promoter and upregulates its expression *in vitro*. (Supports Figure 1)

(A) Diagram of *MYB16* genome region. Arrow heads indicate SPCH-binding peaks obtained from SPCH ChIP-seq data (Lau et al., 2014) as shown in **Figure 1D**. The five amplicons (black bars) were designed for the ChIP-qPCR assay in **(B)**.

(B) MUTE binds to the defined *MYB16* promoter region as does SPCH. 4-dpg *MUTEp:MUTE-CFP* seedlings were used to perform ChIP-qPCR by GFP-trap beads. Two biological replicates showed similar results. *EIF4A1* is a negative control. Data are means (SD).

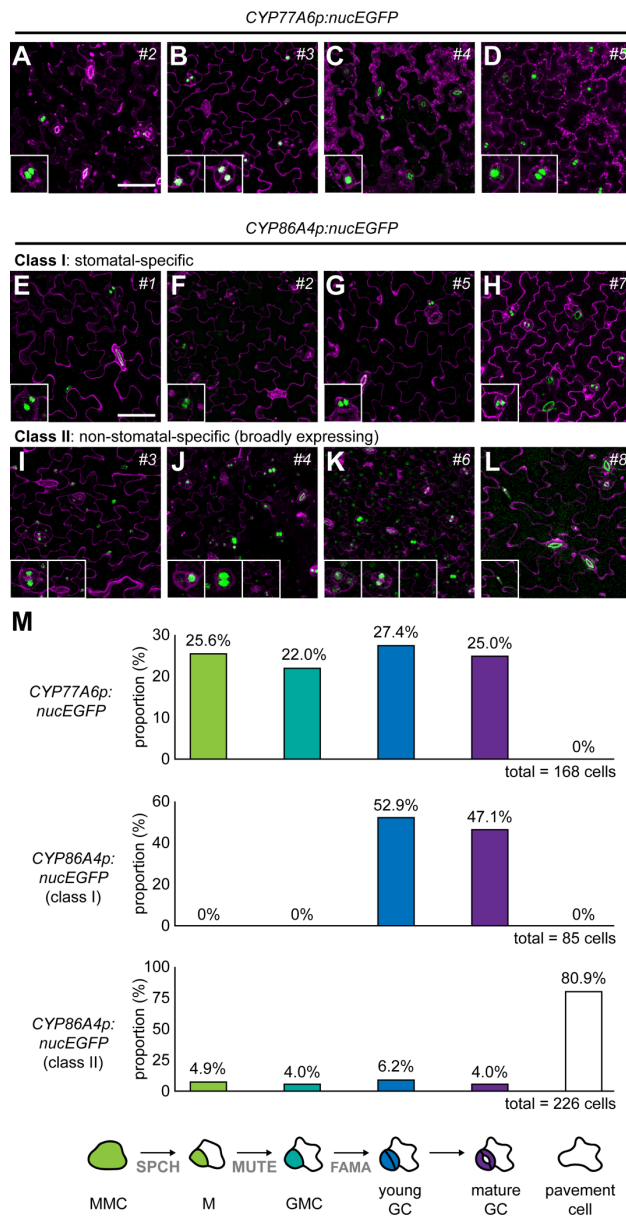
(C) MUTE upregulates *MYB16* expression with SCR1/ICE1. The same *MYB16* reporter and SCR1/ICE1 expression clone were used as shown in **Figure 1F** and **1G**. The luciferase assay was performed in 3-week-old WT protoplasts. Four biological replicates showed similar results. *, $p < 0.001$, by Student's t-test. Data are means (SD).



Supplemental Figure S3. The workflow of the analysis of MYB16 and SPCH dynamics using PrefixSpan. (Supports Figure 4)

(A) Cell states in confocal time-lapse images were defined as 4 categories based on the fluorescence signal and cell plate formation.

(B) Behaviors of the cells were analyzed by the PrefixSpan algorithm. First, the 156 cells with different states were recorded across 7 time points (the time intervals between points are 8 or 16 h). Second, the matrix was applied to the PrefixSpan algorithm with generator patterns (Python). Finally, patterns containing > 1 element in the output matrix were produced. A total of 57 patterns were generated with frequency (number of cells with the designed pattern). The percentage frequency (%) in **Figure 4** was calculated as frequency divided by total cell number (156 cells).



Supplemental Figure S4. Quantification of the *CYP77A6* and *CYP86A4* transcription patterns.

(Supports Figure 4)

(A) to (D) Confocal images of 4 independent T1 lines with *CYP77A6* promoter-driven nuclear enhanced GFP (*CYP77A6p:nucEGFP*). All independent lines show similar results that *CYP77A6* expression is stomatal lineage-specific. The GFP signals were found in meristemoids, guard mother cells and guard cells. 4 of 7 individual lines are shown here.

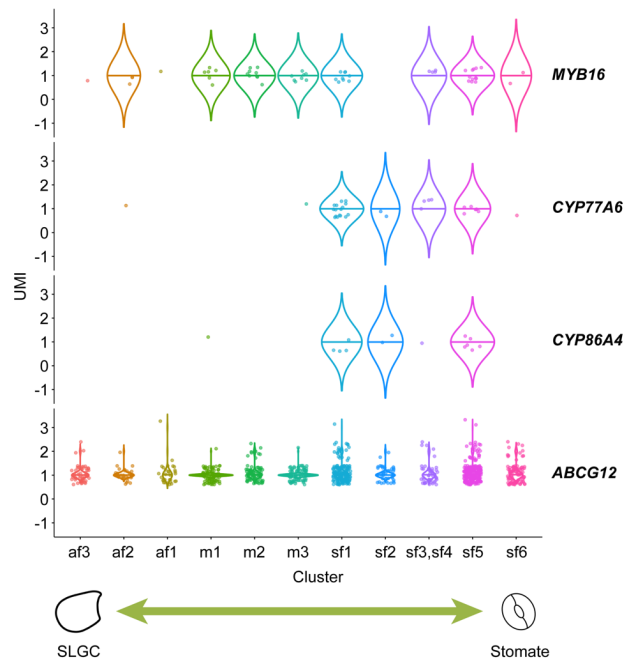
(E) to (L) Confocal images of several independent T1 lines of *CYP86A4p:nucEGFP*. Class I (E) to (H) shows *CYP86A4* expression is guard cell-specific. Class II (I) to (L) shows *CYP86A4* is broadly expressed in all epidermal cells. 8 of 8 individual lines are shown here.

Supplemental Data. Yang et al. (2022). Misregulation of MYB16 expression causes stomatal cluster formation by disrupting polarity during asymmetric cell divisions. Plant Cell.

(M) Quantification of nuclear EGFP signal indicates that *CYP77A6* is specifically expressed in stomatal lineage cells, while *CYP86A4* is either specifically expressed in guard cells (class I) or broadly expressed in epidermal cells (class II). MMC, meristemoid mother cell; M, meristemoid; GMC, guard mother cell; GC, guard cell.

For **(A)** to **(L)**, shared scale bars, 50 μm , in **(A)** and **(E)**. Whole-leaf confocal images of 4-dpg cotyledons and 8-dpg true leaves were used in **(M)**. The quantification was calculated from cells with type-specific signals divided by fluorescence positive cells. Total of 168 cells in **(A)** to **(D)**, 85 cells in **(E)** to **(H)**, and 226 cells in **(I)** to **(L)**.

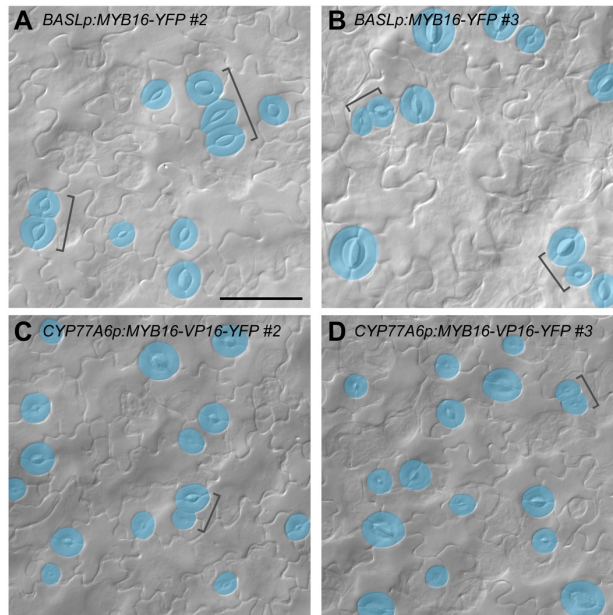
Supplemental Data. Yang et al. (2022). Misregulation of MYB16 expression causes stomatal cluster formation by disrupting polarity during asymmetric cell divisions. Plant Cell.



Supplemental Figure S5. Expression patterns of the MYB16-targeted genes from a single-cell perspective (Lopez-Anido et al., 2021). (Supports Figure 4)

Violin plots show a range of gene expression profiles of *MYB16* and its downstream targets, *CYP77A6*, *CYP86A4* and *ABCG12*. *CYP77A6* and *CYP86A4* transcript levels are higher in cells with stomatal fate. sf, stomatal fate; m, meristemoid; af, alternative fate.

Supplemental Data. Yang et al. (2022). Misregulation of MYB16 expression causes stomatal cluster formation by disrupting polarity during asymmetric cell divisions. Plant Cell.



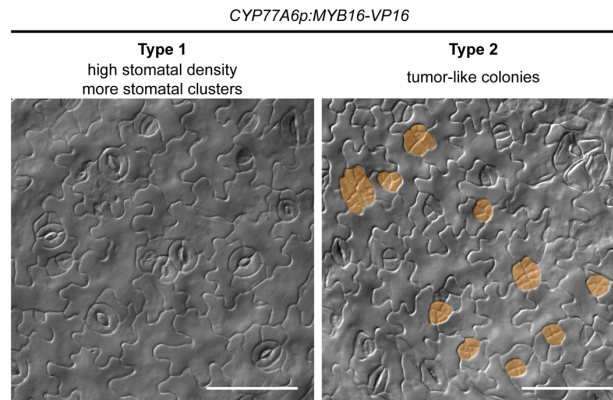
Supplemental Figure S6. The ectopic expression of *MYB16* results in the formation of stomatal clusters. (Supports Figure 4)

(A) and **(B)** DIC images of lower epidermis of 10-dpg *BASLp:MYB16-YFP* cotyledons.

(C) and **(D)** DIC images of lower epidermis of 10-dpg *CYP77A6p:MYB16-VP16-YFP* true leaves.

Different from lines shown in **Figure 4H** and **4I**, 2 of 3 independent lines of each background are shown here. Stomatal clusters are indicated by brackets, and mature guard cells are pseudo-colored in blue. For **(A)** to **(D)**, shared scale bar, 50 μ m, in **(A)**.

Supplemental Data. Yang et al. (2022). Misregulation of MYB16 expression causes stomatal cluster formation by disrupting polarity during asymmetric cell divisions. Plant Cell.

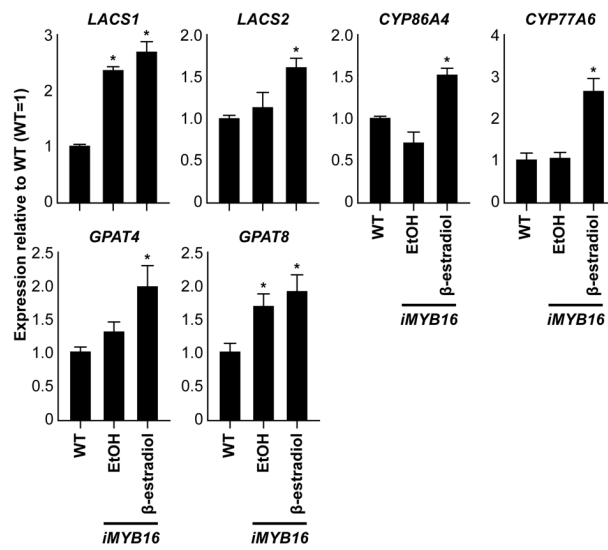


Supplemental Figure S7. Two types of stomatal phenotypes in *CYP77A6p:MYB16-VP16*.

(Supports Figure 4)

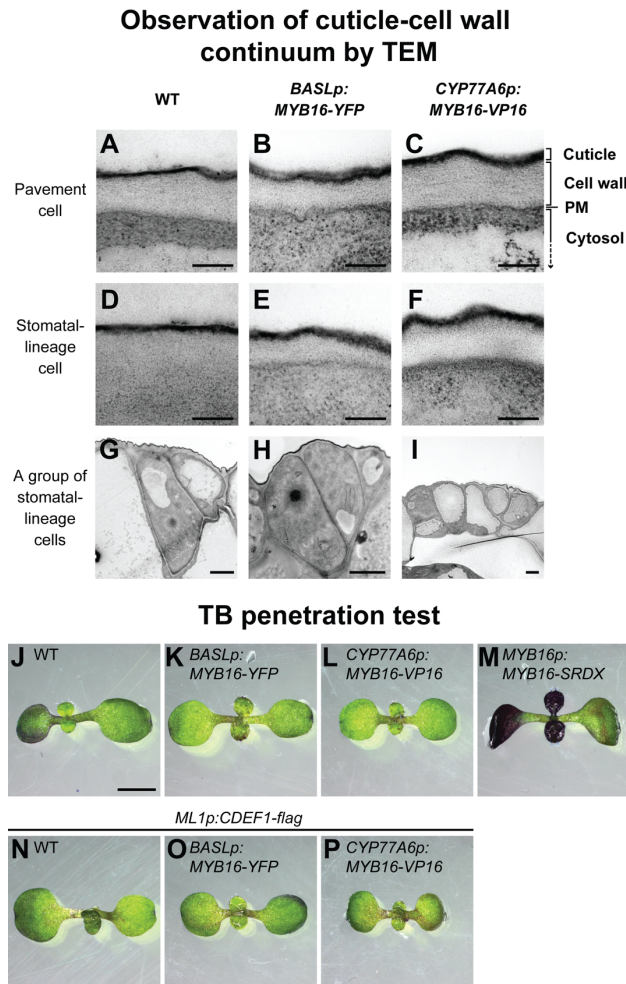
DIC images of 10-dpg true leaves of *CYP77A6p:MYB16-VP16*. Type 1 shows higher density of mature guard cells and more frequent cluster events. Type 2 shows tumor-like colonies (small cell clusters, pseudo-colored in orange) and lower density of mature guard cells, which explains the wide range of stomatal density and index seen in **Figure 4M and 4N**. Scale bars, 50 μ m.

Supplemental Data. Yang et al. (2022). Misregulation of MYB16 expression causes stomatal cluster formation by disrupting polarity during asymmetric cell divisions. Plant Cell.



Supplemental Figure S8. Cutin-related genes are upregulated after induction in the *iMYB16* lines. (Supports Figure 5)

Relative mRNA expression of cuticle biosynthesis genes in the *iMYB16* lines (*iMYB16* #3) with 10-dpg WT as a standard (WT equal to 1). All selected genes for cutin biosynthesis were upregulated after 4 days of 50 μM β-estradiol treatment. *, $p < 0.01$, by Student t-test. Data are means (SD).



Supplemental Figure S9. Phenotypes of ectopic *MYB16* lines revealed by TEM and a TB penetration assay. (Supports Figure 5)

(A) to (F) Images by transmission electron microscopy (TEM) of 7-dpg true leaves of WT (A) and (D), *BASLp:MYB16-YFP* (B) and (E), and *CYP77A6p:MYB16-VP16* (C) and (F). The cuticle (electron-dense region at the top) of pavement cells or stomatal-lineage cells is thicker in *BASLp*- and *CYP77A6p*-driven *MYB16* lines than in WT plants.

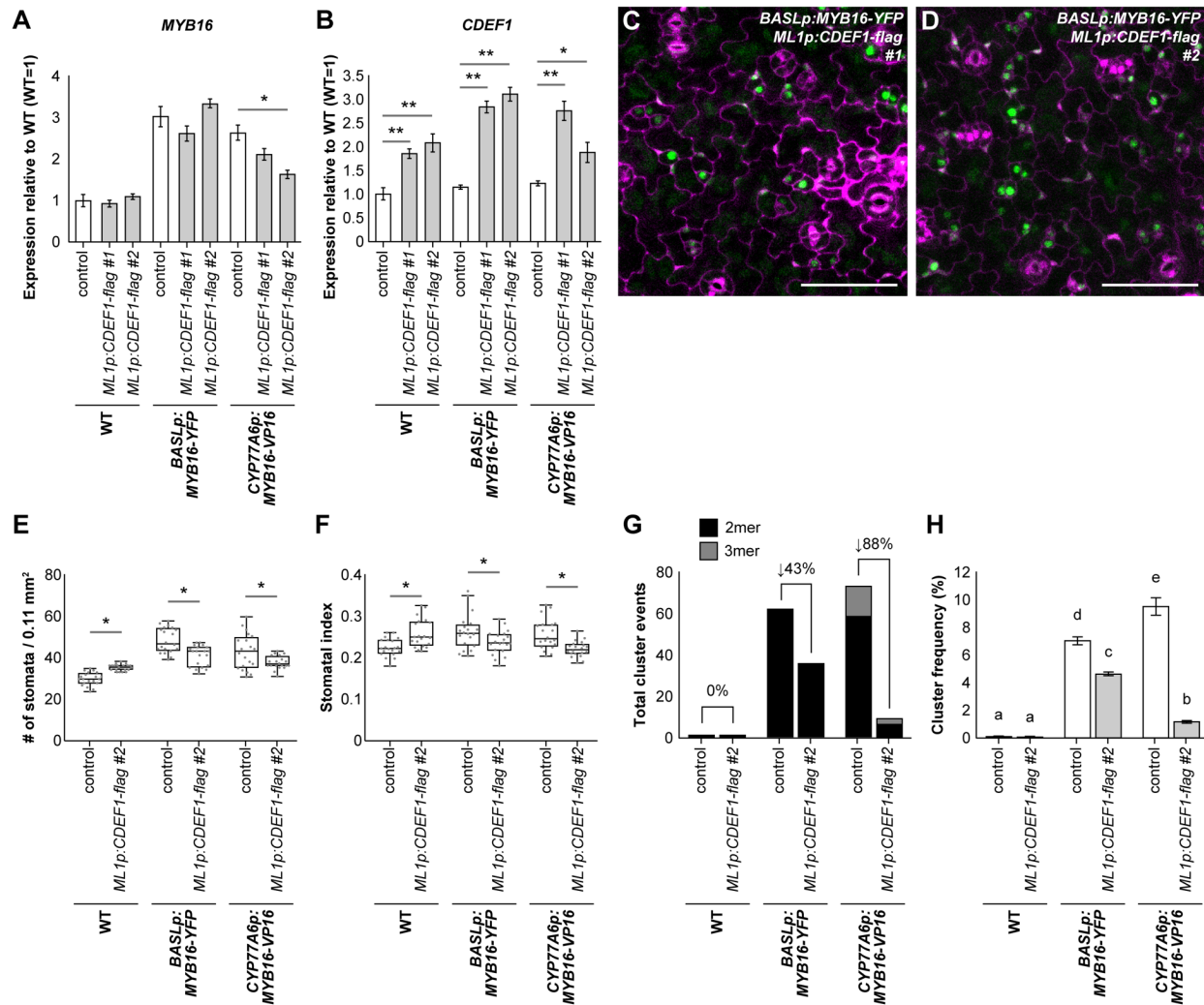
(G) to (I) TEM images focusing on groups of stomatal-lineage cells of 7-dpg true leaves of WT (G), *BASLp:MYB16-YFP* (H) and *CYP77A6p:MYB16-VP16* (I). Abnormally small cell cluster (tumor-like) were found in the *MYB16* ectopic lines, especially in *CYP77A6p:MYB16-VP16*.

(J) to (M) Toluidine blue (TB) test on 7 dpg seedlings of WT, *BASLp:MYB16-YFP*, *CYP77A6p:MYB16-VP16* and *MYB16p:MYB16-SRDX*.

(N) to (P) Toluidine blue (TB) test on 7 dpg seedlings of WT, *BASLp:MYB16-YFP*, *CYP77A6p:MYB16-VP16* after ectopically introducing *CDEF1* into epidermis by *ML1* promoter.

Supplemental Data. Yang et al. (2022). Misregulation of MYB16 expression causes stomatal cluster formation by disrupting polarity during asymmetric cell divisions. *Plant Cell*.

For **(A)** to **(F)**, scale bars represent 200 nm. For **(G)** to **(I)**, scale bars represent 2 μm . For **(J)** to **(P)**, the shared scale bar in **(J)** represents 2 mm.



Supplemental Figure S10. Introducing the cutinase gene *CDEF1* into the leaf epidermis rescues the stomatal phenotype in the ectopic *MYB16* lines. (Supports Figure 5)

(A) and **(B)** Relative mRNA expression of *MYB16* **(A)** and *CDEF1* **(B)**. 7-dpg WT is used as a reference (equal to 1). Both *MYB16* and *CDEF1* were not silent in the double transgenic lines but *MYB16* expression was reduced in *CYP77A6p:MYB16-VP16/ML1p:CDEF1-flag #2*. *, $p < 0.05$; **, $p < 0.01$, by Student's t-test. Data are means (SD).

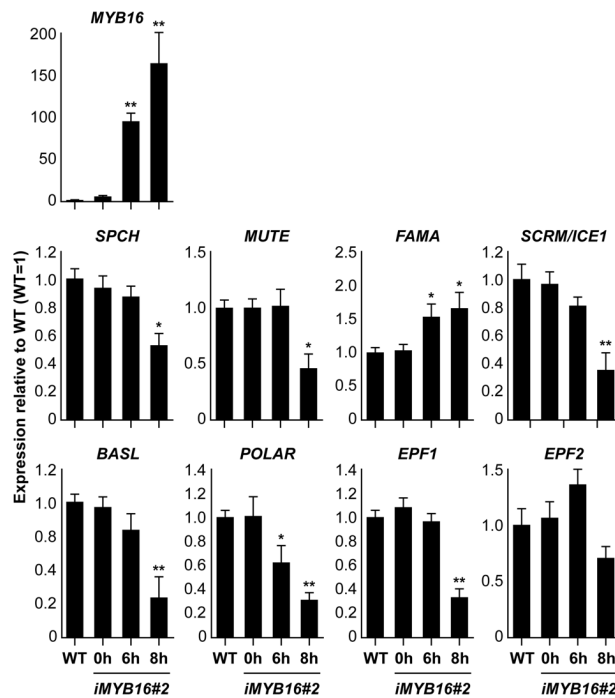
(C) and **(D)** Confocal images of 8-dpg true leaves of *BASLp:MYB16-YFP/ML1p:CDEF1-flag*. Two individual lines show *MYB16-YFP* expression in stomatal lineage cells. Scale bars, 50 μm.

(E) and **(F)** Quantification of stomatal density **(E)** and stomatal index **(F)** by another *CDEF1*-transgenic line #2 in each background show the partial rescue. $n = 20$ 10-dpg seedlings. *, $p < 0.05$, by Wilcoxon signed-rank test. Data are medians (interquartile range).

Supplemental Data. Yang et al. (2022). Misregulation of MYB16 expression causes stomatal cluster formation by disrupting polarity during asymmetric cell divisions. Plant Cell.

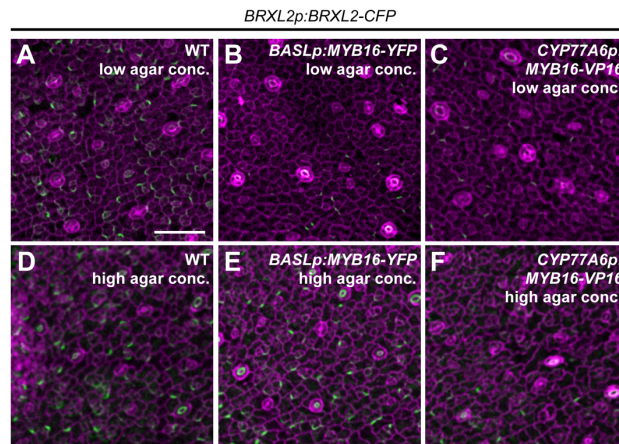
(G) and **(H)** The stomatal clusters **(G)** and cluster frequency **(H)** by CDEF1-transgenic line #2 in each background show cluster reduction. For **(G)**, the value obtained from the sum of the events of 20 lower-epidermis samples. Rescue percentage is the difference of the cluster event between control and *ML1p:CDEF1-flag* divided by the event number in control. For **(H)**, cluster frequency is cluster event number divided by stomatal group number. $p < 0.05$. One-way ANOVA with Tukey post-hoc test. Data are means (SE).

Total 4 individual lines of each background were collected and characterized. Line one (#1) were presented in **Figure 5M** to **5Q**.



Supplemental Figure S11. Expression of genes related to stomatal development in the *iMYB16* lines after a short-term induction of *MYB16* expression, as revealed by qRT-PCR. (Supports Figure 6)

Relative mRNA expression of stomatal development-related genes in 7-dpg WT and *iMYB16* plants after 50 μ M β -estradiol induction. 7-dpg WT is used as a reference (equal to 1). *MYB16* expression was highly upregulated after induction. *SPCH* and *MUTE*, transcription factors (TFs) for cell division and commitment, downregulated after 8 h induction. *FAMA*, TF for stomatal maturation, slightly upregulated after 6 h and 8 h induction. *SCRM/ICE1*, a co-TF working with the *SPCH*, *MUTE* and *FAMA*, downregulated after 8 h induction. *BASL* and *POLAR*, proteins participating in the polarity complex during asymmetric division, downregulated after 8 h and 6 h induction, respectively. EPF peptides trigger inhibitory signaling to prevent stomatal formation in SLGCs. *EPF1* significantly and *EPF2* moderately reduced after 8 h induction. Data are means (SD). *, $p < 0.05$. **, $p < 0.01$.



Supplemental Figure S12. Polarity in the ectopic *MYB16* lines is rescued by growth on high-percentage agar growth medium. (Supports Figure 6 and 7)

(A) to (C) Confocal images of the polarity marker BRXL2 in 7-dpg true leaves of WT (A), *BASLp:MYB16-YFP* #2 (B) and *CYP77A6p:MYB16-VP16* #2 (C) under low-percentage (0.8%) agar treatment.

(D) to (F) Confocal images of the polarity marker BRXL2 in 7-dpg true leaves of WT (A), *BASLp:MYB16-YFP* #2 (B) and *CYP77A6p:MYB16-VP16* #2 (C) under high-percentage (2.4%) agar treatment.

Different from lines shown in **Figure 6** and **7**, 1 of 4 independent lines of each background is shown here. Cell outline is labelled by propidium iodide. Shared scale bar, 50 μ m, in (A).

Supplemental Data. Yang et al. (2022). Misregulation of MYB16 expression causes stomatal cluster formation by disrupting polarity during asymmetric cell divisions. Plant Cell.

Supplemental Table S1. Primers for DNA manipulation.

DNA constructs for luciferase assay

Backbone	Insert	Primer name	Sequence	Enzyme
pJD301	MYB16p	MYB16p-LUCGib-F2	<u>TTGGAGAGAACACGGGGGACAATTTGAGACACATA</u>	NEBuilder
			AACATCTAAG	HiFi
		MYB16p-LUCGib-R	<u>ATGTTTTTGGCATCTCCATTTGTTTTGAGAGCAAAG</u>	NEBuilder
			AAATAAGAACC	HiFi
pENTR/D-TOPO	SPCH	SPCH-F_caccNotI	<u>CACCGCGCCGCATGCAGGAGATAATACCGGATTT</u> TCTTG	NotI
		SPCH_R_AscI	<u>CGGGGCGCGCCCGCAGAATGTTTGCTGAATTTGTT</u> GAGCC	AscI
pENTR/D-TOPO	SCRM/ICE1	SCRM-DTOPO-NotI-F	<u>CACCGCGCCGCCATGGGTCTTGACGGAAACAATG</u> GTG	NotI
		SCRM-CDSns-AscI-R	<u>GTCGGCGCGCCGATCATAACCAGCATAACCTGCTG</u> TATCG	AscI

Note. Underlines in Sequence Column show the recombination or restriction enzyme targeting sites.

DNA constructs for transgenic plants

Backbone	Insert	Primer name	Sequence (Underlines show the enzyme-targeted sites)	Enzyme	Reference
pENTR 5'S		EcoRIcut-NotI_AscI_F	/5Phos/AATTC <u>GCGCGCCGCGCGCGCCG</u>	NotI-AscI	
		EcoRIcut_NotI_AscI_R	/5Phos/AATTC <u>GCGCGCCGCGCGCCG</u>	AscI-NotI	

Supplemental Data. Yang et al. (2022). Misregulation of MYB16 expression causes stomatal cluster formation by disrupting polarity during asymmetric cell divisions. Plant Cell.

pENTR/D-TOPO	<i>MYB16</i>	MYB16F_AT5G15310	CACCATGGGTAGATCACCGTGTGTGAC		
		MYB16R_AT5G15310	GAACATCGGTGAATCCGACGG		
	<i>3×FLAG</i>	3FLAG-Ascl-F	GTGGGCGCGCCGGCATGGATGAACTATACAAAGGTA CC	Ascl	
		3FLAG-Ascl-R	GTCGGGCGGCCAACCAGGCCCCCTCG	Ascl	
pENTR/D-TOPO	<i>CYP77A6p:</i> <i>MYB16-VP16</i>	CYP77A6p-NotI-F	CACCGCGGCCGCTTATCTTCCCGGAATTAGTGAAGAC CC	NotI	
		VP16-Ascl-R	GTCGGGCGGCCCCCCACCGTACTCGTCAATTCCAAG GGCAT	Ascl	
pENTR/D-TOPO	<i>CYP77A6p</i>	CYP77A6p-NotI-F	CACCGCGGCCGCTTATCTTCCCGGAATTAGTGAAGAC CC	NotI	Oshima et al. (2013)
		CYP77A6p-Ascl-R	GTCGGGCGGCCCTTTTAGCTTCTTGTTTTTCTTCTTCT TTTC	Ascl	
pENTR/D-TOPO	<i>CYP86A4p</i>	CYP86A4p-NotI-F	CACCGCGGCCGCTTGTGTGTGGTCCGAAGAAGATG AGA	NotI	Oshima et al. (2013)
		CYP86A4p-Ascl-NotI-R	CACCGCGGCCGCGGCCGCGCCCGTAGCTCTTTTATTA TTGTTTCCCAGAG	Ascl-NotI	
pENTR/D-TOPO	<i>CDEF1</i>	CDEF-NotI-F	CACCGCGGCCGATGGTCGAGGGAGAGTCCAA	NotI	Takahashi et al. (2010)
		CDEF-Ascl-R	GTCGGGCGGCCCATTCACTAACTGGGATATGTTGAA CGG	Ascl	

Supplemental Data. Yang et al. (2022). Misregulation of MYB16 expression causes stomatal cluster formation by disrupting polarity during asymmetric cell divisions. Plant Cell.

pENTR P4-P1R	<i>BRXL2p</i>	At3g14000/BRXL2 proF	<u>GGGACAAC</u> TTTGTATAGAAAAGTTGCGAAACAGATC GTTGTGTAGAGTACC	BP clonase
		At3g14000/BRXL2 proR	GGGACTGCTTTTTTGTACAAACTTGCTCTATCACTC ACTAAAGAGTTTCAATTTTCG	BP clonase

Note. Underlines in Sequence Column show the recombination or restriction enzyme targeting sites.

Supplemental Data. Yang et al. (2022). Misregulation of MYB16 expression causes stomatal cluster formation by disrupting polarity during asymmetric cell divisions. *Plant Cell*.

Supplemental Table S2. Details of DNA manipulation.

DNA constructs for reporters

Construct	Entry vectors (inserts)	Destination vectors	Reference
<i>iMYB16</i>	pENTR/D-TOPO (MYB16-3×flag) ^[2]	pCAMBIA1390(GW) ^[2]	modified from Kubo et al., (2013)
<i>CYP86A4p:nucEGFP</i>	pENTR/D-TOPO (CYP86A4p)	pBGGN	Kubo et al. (2005)
<i>CYP77A6p:nucEGFP</i>	pENTR/D-TOPO (CYP77A6p)	pBGGN	Kubo et al. (2005)
<i>MYB16p:MYB16-YFP</i>	pDONR P4-P1R (MYB16p) pENTR/D-TOPO (MYB16)	R4pGWB540	Oshima et al. (2013) Nakagawa et al. (2008)
<i>BASLp:MYB16-YFP</i>	pENTR 5'-TOPO (BASLp) pENTR/D-TOPO (MYB16)	R4pGWB540	Dong et al. (2009) Nakagawa et al. (2008)
<i>CYP77A6p:MYB16-VP16-YFP</i>	pENTR/D-TOPO (CYP77A6p:MYB16-VP16)	pHGY	Oshima and Mitsuda (2016) Kubo et al. (2005)
<i>AtML1p:CDEF1-flag</i>	pDONR P4-P1R (AtML1p) pENTR/D-TOPO (CDEF1)	R4pGWB610	Davies and Bergmann (2014) Nakagawa et al. (2008)
<i>BRXL2p:BRXL2-CFP</i>	pENTR P4-P1R (BRXL2p) pENTR/D-TOPO (BRXL2)	R4pGWB443	Rowe et al. (2019) Nakagawa et al. (2008)
<i>35S:SPCH-YFP</i>	pENTR/D-TOPO (SPCH)	pH35GY	Lampard et al. (2008) Kubo et al. (2005)
<i>35S:SCRM/ICE1-CFP</i>	pENTR/D-TOPO (SCRM/ICE1)	pH35GC	Kubo et al. (2005)

Supplemental Data. Yang et al. (2022). Misregulation of MYB16 expression causes stomatal cluster formation by disrupting polarity during asymmetric cell divisions. *Plant Cell*.

DNA constructs for luciferase assay and CRISPR-Cas9 editing

Construct	Description	Reference
<i>Mini35S-MYB16p:LUC2</i>	~3 kb MYB16 promoter was inserted into pJD301 containing <i>mini35S:LUC2</i> and	Luehrsen et al. (1992)
	<i>UBQ10p:hREN</i> by KpnI (NEB) and HiFi DNA Assembly Master Mix (NEB).	
<i>Myb16-crispr</i>	For generation of <i>myb16-crispr</i> lines, the guide RNA (gRNA), GACAAATTGGGTTTGAAGAA was	Yan et al. (2015)
	introduced into plasmid containing AtU6-26-sgRNA by BsaI (NEB). The fragment was then	
	introduced into pCAMBIA1300-221 containing <i>YAOp:Cas9</i> by SpeI and NheI.	

Note. 1) Constructs were created by Gateway (Invitrogen) cloning with pENTR 5'-TOPO, pENTR/D-TOPO and pDONR P4-P1R plasmids as backbones. To facilitate cloning processes, we modified pENTR 5'-TOPO by EcoRI (NEB) to introduce NotI and Ascl sites; the resulting plasmid was called pENTR 5'S. Genes were cloned into pENTR/D-TOPO plasmids by using conventional TOPO isomerase (Invitrogen) or by restriction enzyme digestion with NotI and Ascl (NEB) depending on the primer design listed in Supplemental Table S1.

2) pCAMBIA1390(GW) containing 35S:XVE-LexA, a gift from Dr. Shih-Long Tu's lab (IPMB, Academia Sinica). 3×flag fragment was obtained using modified pCAMBIA1390(HA-GFP-FLAG) (Wu et al., 2016) as a backbone.

Supplemental Data. Yang et al. (2022). Misregulation of MYB16 expression causes stomatal cluster formation by disrupting polarity during asymmetric cell divisions. *Plant Cell*.

Supplemental Table S3. Details of plant materials.

Mutant or transgenic line	Description
<i>myb16-crispr</i>	Generated by introducing pCAMBIA1300-221 containing <i>YAOp:Cas9</i> and the small guide RNA (sgRNA) driven by the <i>AtU6</i> promoter (Yan et al., 2015). After selection to Cas9-free T4 plants, the plants were used for phenotyping.
<i>amiR-MYB16/</i> <i>myb106-2</i>	Oshima et al., 2013. 2 independent lines were characterized.
<i>MYB16p:MYB16-YFP;</i> <i>SPCHp:SPCH-CFP;</i> <i>ML1p:RC12A-mCherry</i>	Transgenic line expressing three markers. Generated by crossing <i>MYB16p:MYB16-YFP</i> (Ho et al., 2021) and <i>SPCHp:SPCH-CFP; ML1p:RC12A-mCherry</i> (Davies and Bergmann, 2014).
<i>SPCHp:SPCH-CFP</i>	Davies and Bergmann, 2014.
<i>MUTEp:MUTE-CFP</i>	Davies and Bergmann, 2014.
<i>iMYB16</i>	Transgenic line containing <i>35S:XVE</i> and <i>LexAp:MYB16-3xflag</i> to overexpress <i>MYB16</i> under β -estradiol treatment. 4 independent lines (T3) were isolated and characterized.
<i>CYP77A6p:nucEGFP</i>	Transgenic line expressing nucEGFP under the control of the <i>CYP77A6</i> promoter. 7 independent lines (T1) were isolated and characterized.
<i>CYP86A4p:nucEGFP</i>	Transgenic line expressing nucEGFP under the control of the <i>CYP86A4</i> promoter. 8 independent lines (T1) were isolated and characterized.

Supplemental Data. Yang et al. (2022). Misregulation of MYB16 expression causes stomatal cluster formation by disrupting polarity during asymmetric cell divisions. Plant Cell.

<i>BASLp:MYB16-YFP</i>	Transgenic line expressing MYB16 under <i>BASL</i> promoter to ectopically introduce MYB16 during asymmetric division. 3 independent lines (T1 to T4) were isolated and characterized.
<i>CYP77A6p:MYB16-VP16</i>	Oshima and Mitsuda, 2016.
<i>CYP77A6p:MYB16-VP16-YFP</i>	Transgenic line derived from <i>CYP77A6p:MYB16-VP16</i> (Oshima and Mitsuda, 2016) by adding a fluorescent tag at C-terminal region of VP16. 2 independent lines (T3 and T4) were isolated and characterized.
<i>BASLp:MYB16-YFP</i> ; <i>ML1p:RC12A-mCherry</i>	Transgenic line expressing two markers. Generated by crossing <i>BASLp:MYB16-YFP</i> and <i>ML1p:RC12A-mCherry</i> (Davies and Bergmann, 2014).
<i>BRXL2p:BRXL2-CFP</i>	Transgenic line expressing <i>BRXL2</i> polarity marker under native promoter. 4 independent lines (T2) were isolated and characterized.
<i>BRXL2p:BRXL2-CFP</i> ; <i>BASLp:MYB16-YFP</i>	Transgenic line expressing <i>BRXL2</i> polarity marker under native promoter. Generated by transforming <i>BRXL2p:BRXL2-CFP</i> into <i>BASLp:MYB16-YFP</i> background. 4 independent lines (T2) were isolated and characterized.
<i>BRXL2p:BRXL2-CFP</i> ; <i>CYP77A6p:MYB16-VP16</i>	Transgenic line expressing <i>BRXL2</i> polarity marker under native promoter. Generated by transforming <i>BRXL2p:BRXL2-CFP</i> into <i>CYP77A6p:MYB16-VP16</i> background. 4 independent lines (T2) were isolated and characterized.
<i>ML1p:CDEF1-flag</i>	Transgenic line ectopically expressing <i>CDEF1</i> cutinase under epidermal-specific promoter. 5 independent lines (T2) were isolated and 4 of them were characterized.
<i>ML1p:CDEF1-flag</i> ; <i>BASLp:MYB16-YFP</i>	Transgenic line ectopically expressing <i>CDEF1</i> cutinase under epidermal-specific promoter. Generated by transforming <i>ML1p:CDEF1-flag</i> into <i>BASLp:MYB16-YFP</i> background. 5 independent lines (T2) were isolated and 4 of them were characterized.

Supplemental Data. Yang et al. (2022). Misregulation of MYB16 expression causes stomatal cluster formation by disrupting polarity during asymmetric cell divisions. *Plant Cell*.

<i>ML1p:CDEF1-flag;</i> <i>CYP77A6p:MYB16-VP16</i>	Transgenic line ectopically expressing <i>CDEF1</i> cutinase under epidermal-specific promoter. Generated by transforming <i>ML1p:CDEF1-flag</i> into <i>CYP77A6p:MYB16-VP16</i> background. 5 independent lines (T2) were isolated and 4 of them were characterized.
<i>35Sp:EPF2</i>	Transgenic line overexpressing <i>EPF2</i> under the control of the 35S promoter. 20 independent lines (T1) were isolated and characterized.
<i>35Sp:EPF2;</i> <i>BASLp:MYB16-YFP</i>	Transgenic line overexpressing <i>EPF2</i> under 35S promoter. Generated by transforming <i>35Sp:EPF2</i> into <i>BASLp:MYB16-YFP</i> background. 20 independent lines (T1) were isolated and characterized.

Note. All mutants and transgenic lines were in the Col-0 background.

Supplemental Table S4. Primers used in this study.

qRT PCR: mRNA expression level

Gene	Forward/Reverse	Sequence
<i>MYB16</i>	Forward	TTGGACAACAAAACACACGAAG
	Reverse	TGTAGATGTCGGAGATTCAAGCT
<i>LACS1</i>	Forward	TGGAGACAAAACCTTTCGACGT
	Reverse	TGAGCGTCGCAGTCACTAAGTC
<i>LACS2</i>	Forward	CTCAAGATGTCCCCTCATTGC
	Reverse	GACTCGAAGCTGTTGCCATAGA
<i>CYP86A4</i>	Forward	CCGCTCTTGAATTCACAACAAG
	Reverse	GTTCTGCATTGTCTTGAGCCGTTGC
<i>CYP77A6</i>	Forward	CGAAGAAATTTAACCCGGATCG
	Reverse	TATGTCCGCTTCCTCCTTACCC
<i>GPAT4</i>	Forward	CGATTTTCATGTCCATTTGCAAG
	Reverse	GGCTGATTTGGTCTCATGCACC
<i>GPAT8</i>	Forward	GCCAACATGAGAAAACCTTCTCG
	Reverse	CGTCGTGCCTTCCGGACATATC
<i>CDEF1</i>	Forward	AACCGGTCGGTTTAGCAAC
	Reverse	GCTTGTGCCTGTGATGCTC
<i>SPCH</i>	Forward	ATCATAGGAGGAGTTGTGGAG
	Reverse	TAGAACAGGCGGTGAAGGAC
<i>MUTE</i>	Forward	CGATCATCGGAGGAGTGATAGA
	Reverse	AAGGGAAAGATGGTCGGTTTAG
<i>FAMA</i>	Forward	GAACAAACCGTCCTCTACTCC
	Reverse	ATATTTCCCAGGTTAGAGCTTCC
<i>SCRM1/ICE1</i>	Forward	ACACCTACACCGCAAACCTC
	Reverse	TCTACGACCACAGAACATATGAATG
<i>BASL</i>	Forward	AGACGGAATCGTCCTCGGAA
	Reverse	CCTTGACATGAAGTGTTATCG
<i>POLAR</i>	Forward	CCTGAATAAGAGTAAAGAGCCGG
	Reverse	GCATTCGCAGGTTTGTTCATC

Supplemental Data. Yang et al. (2022). Misregulation of MYB16 expression causes stomatal cluster formation by disrupting polarity during asymmetric cell divisions. *Plant Cell*.

<i>EPF1</i>	Forward	CTTGGCTAGGCATTTACCAACA
	Reverse	CAATGCCCCGGTCATTCTTA
<i>EPF2</i>	Forward	TTTGGTCGTTAACTCCATTTCGC
	Reverse	CTTTTCTCCGCCATTGACCGT

ChIP-qRT PCR

Gene (promoter region)	Forward/Reverse	Sequence
<i>MYB16p</i> (region 1)	Forward	AGGCTAACTTGAAGTATGTAAGGACCATAC
	Reverse	AAGAAGAGAGAGGAAGAGAGCTCATGGATC
<i>MYB16p</i> (region 2)	Forward	TGTAAAATCTCTTTAATGTCACCGTTTGCC
	Reverse	ACCTCATCTTGTGATCTTATATGGTTGTGG
<i>MYB16p</i> (region 3)	Forward	GAAGCTAGCTAACAAACCAAGGCATC
	Reverse	CAGCTTCTAGCACTCTAATATCTTCATCCG
<i>MYB16p</i> (region 4)	Forward	TGAGCCGGGAAAAAGGGATTC
	Reverse	GGCTACAGTTGTGGAAATGTTACAAGTG
<i>MYB16p</i> (region 5)	Forward	TTGGACAACAAAACACACGAAG
	Reverse	TGTAGATGTCGGAGATTCAAGCT
<i>EIF4A1</i>	Forward	TGTTTTGCTTCGTTTCAAGGATTCCTC
	Reverse	GCATTTTCCCGATTACAACGAGG

CRISPR: guide RNA (gRNA)

Gene	Forward/Reverse	Sequence
MYB16-gRNA	Forward	ATTGACAAATTGGGTTTGAAGAA
	Reverse	AAACTTCTTCAAACCAATTTGT

Supplemental Data. Yang et al. (2022). Misregulation of MYB16 expression causes stomatal cluster formation by disrupting polarity during asymmetric cell divisions. *Plant Cell*.

Supplemental References

- Davies, K.A. and Bergmann, D.C.** (2014). Functional specialization of stomatal bHLHs through modification of DNA-binding and phosphoregulation potential. *Proc. Natl. Acad. Sci. USA* **111**: 15585–15590.
- Dong, J., MacAlister, C.A., and Bergmann, D.C.** (2009). BASL controls asymmetric cell division in *Arabidopsis*. *Cell* **137**: 1320–1330.
- Ho, C.K., Bringmann, M., Oshima, Y., Mitsuda, N., and Bergmann, D.C.** (2021). Transcriptional profiling reveals signatures of latent developmental potential in *Arabidopsis* stomatal lineage ground cells. *PNAS* **118**: e2021682118.
- Kubo, M., Imai, A., Nishiyama, T., Ishikawa, M., Sato, Y., Kurata, T., Hiwatashi, Y., Reski, R., and Hasebe, M.** (2013). System for stable β -estradiol-inducible gene expression in the moss *Physcomitrella patens*. *PLoS One* **8**: e77356.
- Kubo, M., Udagawa, M., Nishikubo, N., Horiguchi, G., Yamaguchi, M., Ito, J., Mimura, T., Fukuda, H., and Demura, T.** (2005). Transcription switches for protoxylem and metaxylem vessel formation. *Genes Dev.* **19**: 1855–1860.
- Lampard, G.R., MacAlister, C.A., and Bergmann, D.C.** (2008). *Arabidopsis* stomatal initiation is controlled by MAPK-mediated regulation of the bHLH SPEECHLESS. *Science* **322**: 1113–1116.
- Lau, O.S., Davies, K.A., Chang, J., Adrian, J., Rowe, M.H., Ballenger, C.E., and Bergmann, D.C.** (2014). Direct roles of SPEECHLESS in the specification of stomatal self-renewing cells. *Science* **345**: 1605–1609.

Supplemental Data. Yang et al. (2022). Misregulation of MYB16 expression causes stomatal cluster formation by disrupting polarity during asymmetric cell divisions. *Plant Cell*.

Lopez-Anido, C.B., Vatén, A., Smoot, N.K., Sharma, N., Guo, V., Gong, Y., Anleu Gil, M.X.,

Weimer, A.K., and Bergmann, D.C. (2021). Single-cell resolution of lineage trajectories in the *Arabidopsis* stomatal lineage and developing leaf. *Dev. Cell* **56**: 1043–1055.

Luehrsen, K.R., de Wet, J.R., and Walbot, V. (1992). Transient expression analysis in plants using firefly luciferase reporter gene. *Methods Enzymol.* **216**: 397–414.

Nakagawa, T., Nakamura, S., Tanaka, K., Kawamukai, M., Suzuki, T., Nakamura, K., Kimura, T., and Ishiguro, S. (2008). Development of R4 gateway binary vectors (R4pGWB) enabling high-throughput promoter swapping for plant research. *Biosci. Biotechnol. Biochem.* **72**: 624–629.

Oshima, Y. and Mitsuda, N. (2016). Enhanced cuticle accumulation by employing MIXTA-like transcription factors. *Plant Biotechnol.* **33**: 161–168.

Oshima, Y., Shikata, M., Koyama, T., Ohtsubo, N., Mitsuda, N., and Ohme-Takagi, M. (2013). MIXTA-like transcription factors and WAX INDUCER1/SHINE1 coordinately regulate cuticle development in *Arabidopsis* and *Torenia fournieri*. *Plant Cell* **25**: 1609–1624.

Rowe, M.H., Dong, J., Weimer, A.K., and Bergmann, D.C. (2019). A plant-specific polarity module establishes cell fate asymmetry in the *Arabidopsis* stomatal lineage. bioRxiv: doi: 10.1101/614636.

Takahashi, K., Shimada, T., Kondo, M., Tamai, A., Mori, M., Nishimura, M., and Hara-Nishimura, I. (2010). Ectopic expression of an esterase, which is a candidate for the unidentified plant cutinase, causes cuticular defects in *Arabidopsis thaliana*. *Plant Cell Physiol.* **51**: 123–131.

Wu, J.F., Tsai, H.L., Joanito, I., Wu, Y.C., Chang, C.W., Li, Y.H., Wang, Y., Hong, J.C., Chu, J.W., Hsu, C.P., and Wu, S.H. (2016). LWD-TCP complex activates the morning gene CCA1 in *Arabidopsis*. *Nat. Commun.* **7**: 13181.

Supplemental Data. Yang et al. (2022). Misregulation of MYB16 expression causes stomatal cluster formation by disrupting polarity during asymmetric cell divisions. *Plant Cell*.

Yan, L., Wei, S., Wu, Y., Hu, R., Li, H., Yang, W., and Xie, Q. (2015). High-efficiency genome editing in *Arabidopsis* using YAO promoter-driven CRISPR/Cas9 system. *Mol. Plant* **8**: 1820–1823.